

Method of carbon-based electrode analysis by conductive-atomic force microscopy

Ł. Majchrzycki^{1,2}, M. Nowicki¹, R. Czajka¹, K. Lota²

¹*Institute of Physics, Poznan University of Technology, Nieszawska 13a, Poznan 60-965, Poland*

²*Central Laboratory of Batteries and Cells, Institute of Non-ferrous Metals Division in Poznan, Forteczna 12, Poznan 61-362, Poland*

E-mail: lukasz.majchrzycki@gmail.com

Published in Micro & Nano Letters; Received on 18th November 2013; Accepted on 20th December 2013

A novel method of the characterisation of composite materials for electrochemical capacitor electrodes by conductive-atomic force microscopy is reported. The method allowed the analysis of the structure and the distribution of the non-conductive or less conductive additives dispersed in the carbon conductive matrix, which affect the surface conductivity of the electrodes. The composites of activated carbon with nickel (II) oxide, as well as activated carbon or carbon nanotubes with three different conducting polymers – polyaniline, poly(3,4-ethylenedioxythiophene) and polypyrrole – were prepared and tested and analysed by the reported method.

1. Introduction: Electrochemical capacitors (also called supercapacitors or ultracapacitors) are devices developed to store and deliver electrical energy in high-power pulses. They are characterised by high-power density, high efficiency and long shelf and cycle life. In a typical electric double layer (EDL), the supercapacitors' energy is stored as a charge separated in a double layer, which is formed at the interface of the carbon electrode and the electrolyte. Materials such as activated carbon [1], mesoporous carbon [2] and carbon nanotubes (CNTs) [3] are usually used because of their good electrical conductivity and chemical and thermal stability. However, the capacitance of EDL supercapacitors is limited by the microstructure of the electrode. It can be increased by a pseudo-capacitive charge storage mechanism [4] because of the fast surface redox reactions on electroactive materials. A pseudo-capacitive effect can occur, for example, in transition metal oxides [5] and conducting polymers [6, 7]. Recently, polyaniline – PANI [8–10], poly(3,4-ethylenedioxythiophene) – PEDOT [11–13] and polypyrrole – PPy [14–17] composites with various carbon materials were extensively investigated as good candidates for supercapacitor electrodes. The appropriate morphology of the composite and the carbon/polymer ratio has a significant effect on the electrochemical properties of these materials. A high specific surface area (in the range of hundreds m² per gram) gives the possibility to obtain a high Coulomb capacity at the EDL [18, 19]. However, in the pseudo-capacitive additives such as transition metal oxides or electrically conducting polymers, not only the surface but also the total mass and the volume of the material participated in the charge storage [14], hence their morphology, homogeneity of distribution and electrical contact are essential.

It is known that the methods of preparation of a filler and a matrix and the technique of their mixing determine the properties of the composite. In the case of the CNT/polymer composite, the addition of only a small amount of CNT can drastically increase the electrical conductivity of such nanocomposites by the formation of a conductive CNTs network in a polymer matrix [20]. The conductivity of such composites is limited by the contact resistance between the CNTs which can be influenced by the thickness of the insulating polymer layers that cover the CNTs which specifies the tunnelling resistance between the two nanotubes [21, 22]. A tool providing the possibility of nanometre resolution analysis of the carbon/polymer composite structure could be conductive-atomic force microscopy (C-AFM) [20, 23]. By means of this technique, in a more efficient way than by the other scanning probe microscopy modes, the organisation of the carbon materials inside a composite can be

determined. The structure of the composite can be analysed in the context of the carbon paths which are connected into the conductive network and therefore participate in the process of the electrons transfer.

Here, we report a C-AFM-based method of the analysis of the carbon-based composites organisation, which allows us to analyse the content of the less conductive filler and its distribution. In particular, it can extend the analysis capabilities of the electrochemical capacitor electrodes, filling the gap of the lack of methods for the pseudo-capacitive additives distribution examination.

2. Materials and methods: The method was tested by several types of nanocomposite electrodes. Measured electrodes were designed for the asymmetric electrochemical capacitors. The first approach has been performed by using electrodes consisting of 5% carbon black, 10% of binder (PVDF, Kynar Flex 2801) and active material which was a composite of the activated carbon (AC, NORIT[®] SX2) and nickel oxide. As a second approach, the unmixed composites of carbon [AC or multiwalled CNTs (MWNTS)] and the conducting polymers (PANI, PEDOT and PPy) have been used. All these materials were compressed into thin pellets.

2.1. Preparation of the AC/NiO composites: The AC/NiO composite was obtained by a chemical method by the direct precipitation of nickel hydroxide onto activated carbon from the Ni(NO₃)₂ solution by NaOH. The molar ratio of Ni(NO₃)₂ and NaOH was 1:2. The precipitation material was washed and dried at 80°C and at the next step was calcination at 300°C at an air atmosphere for 2 h. The X-ray diffraction analysis (not shown in this Letter) confirmed the full conversion of the precipitate from nickel hydroxide (β-Ni(OH)₂) to nickel (II) oxide (NiO). The amount of NiO at the composite was 17%. For comparison, another composite was obtained by a mechanical method of simple mixing of the AC and the NiO components in the same ratio in a mortar.

2.2. Preparation of the carbon/polymer composites: Carbon/polymer composites have been obtained by a polymerisation of the suitable monomers in the presence of the carbon materials. Activated carbon (AC, NORIT[®] SX2) and MWNTS with a diameter of 110–170 nm and length of 5–9 μm and purity 90+% (Sigma-Aldrich[®]), respectively, were used as the carbon materials.

Carbon/PANI composites were obtained by aniline polymerisation in an acid solution. In particular, aniline (2 ml) was dissolved in 1 M HCl. Next, 1 g of a proper carbon material was added. The mixture underwent vigorous stirring. Excess of the K₂CrO₄ oxidant was

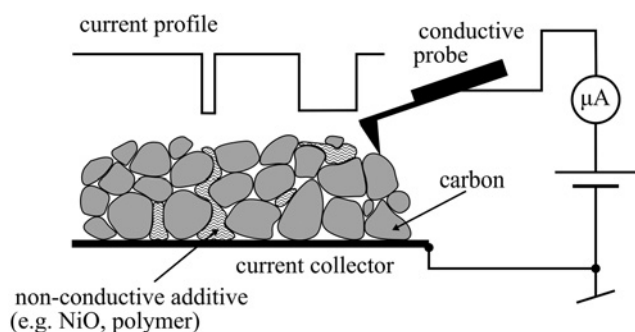


Figure 1 Sketch of C-AFM experimental setup

dissolved in 100 ml of 1 M HCl and added dropwise under vigorous stirring. The polymerisation took 2 h. After that, the composite was washed out by distilled water to remove the residual oxidant until the pH became neutral. The composite was dried at room temperature for 24 h.

The synthesis of the carbon/PEDOT composites was conducted in acetonitrile solvent. One gram of carbon material was added to the monomer PEDOT (1 M solution in acetonitrile), and the mixture was vigorously stirred. An exact amount of the $\text{Fe}(\text{ClO}_4)_3$ oxidant (25%) solution in acetonitrile was added dropwise under vigorous stirring. The product was washed by acetonitrile and dried at room temperature for 24 h after 2 h of polymerisation.

Carbon/PPy composites were obtained similarly to carbon/PANI composites. Pyrrole as a monomer and iron (III) chloride as an oxidant were used. In particular, 1.4919 g of pyrrole was dissolved into 100 ml of chilled 0.1 M HCl solution. 0.5133 g of carbon material was added to the solution and the mixture was vigorously stirred. An exact amount of the FeCl_3 oxidant (10.7379 g) was dissolved in 0.1 M HCl solution and added dropwise to the above solution. After 2 h of polymerisation, the product was washed with distilled water and dried at room temperature for 24 h.

In all the cases, the percentage of the carbon material was in the range of 40–60% depending on the sample which is over the percolation threshold.

2.3. Atomic force microscopy (AFM) measurements: AFM imaging was performed by using the Easy Scan 2 AFM (Nanosurf) in the C-AFM mode and using the Innova scanning probe microscope (Bruker) in the TappingMode[®]. A sketch of the C-AFM experimental setup is shown in Fig. 1. The force of the cantilever-sample interaction during the experiment was kept as low as possible and it did not exceed 5 nN. This value of a force allows for non-destructive surface analysis. The topography and the C-AFM current map were measured simultaneously. The macroscopic bulk sample of the nanocomposite pellet was fixed and connected to the ground. The bias voltage was applied between the conductive tip and the sample and set at 100 mV. The circuit was protected by a 100 kΩ resistor connected in series and the current did not exceed 1 μA. Pt/Ir coated PPP-ContPt probes (NanosensorsTM) were used. All the AFM data analysis was performed by WSxM software [24].

3. Results and discussion: We measured the unadulterated carbon materials for further comparison with our measurement results. The structure of the AC surface is shown in Fig. 2. The porosity of the AC is clearly noted. In the range of tens and hundreds of nanometres, the pores can be imaged by AFM and in the range of several nanometres by a scanning tunnelling microscope (STM). The transmission electron microscopy (TEM) image of the used CNTs is shown in Fig. 3 and the AFM image of the single nanotube at the mica surface is shown in Fig. 6a. Their dimensions are in good agreement with the producer data. The

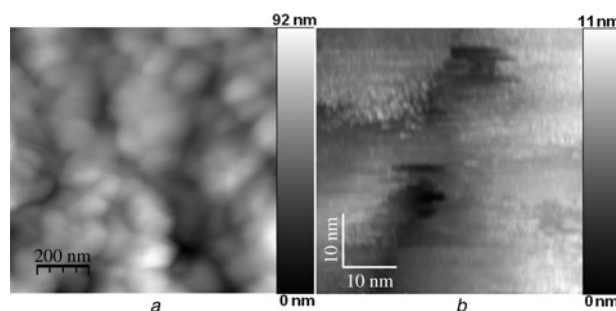


Figure 2 AFM topography of AC surface (Fig. 2a) and STM image of single micropore (Fig. 2b)

declared dimensions are 110–170 nm in diameter and 5–9 μm in length, respectively.

3.1. Structure of the AC/NiO composites: The topographies and the C-AFM current maps of the AC/NiO composites obtained by chemical

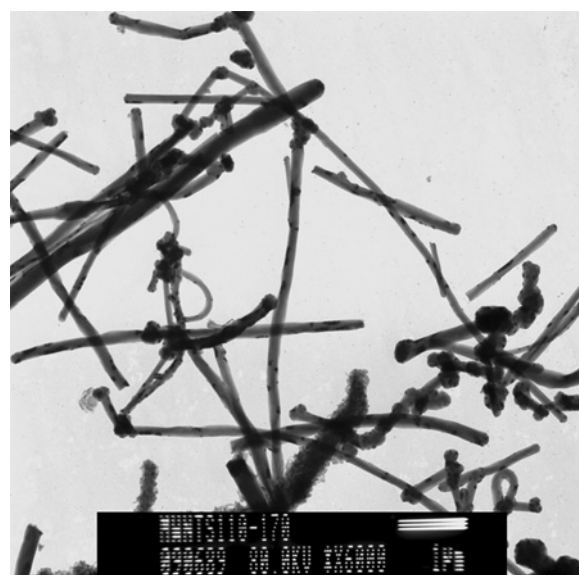


Figure 3 TEM image of multiwalled CNTs of 110–170 nm diameter

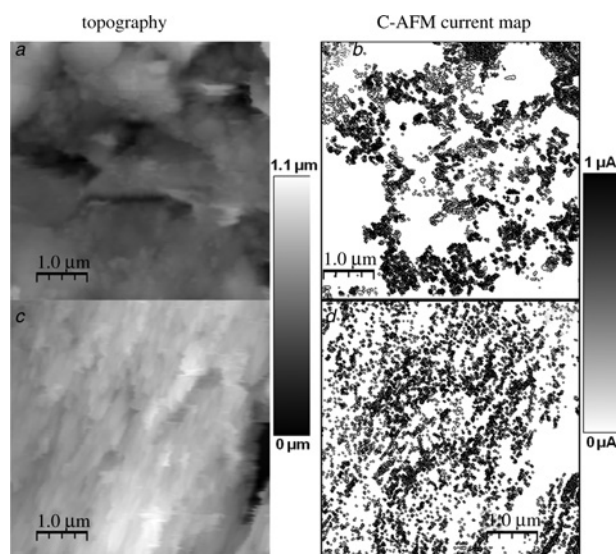


Figure 4 Topographies (Figs. 4a, c) and C-AFM current maps in inverted scale (Figs. 4b, d) of AC/NiO composites obtained by chemical (Figs. 4a, b) and mechanical (Figs. 4c, d) way

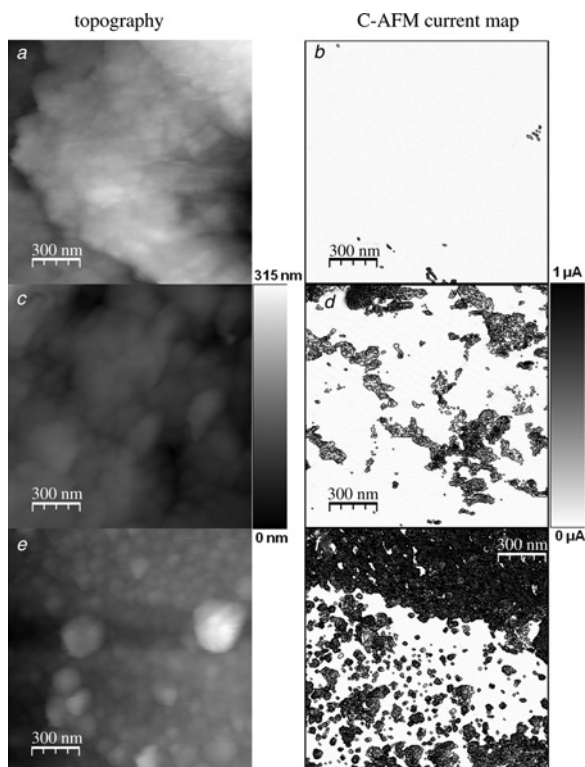


Figure 5 Topographies (Figs. 5a, c, e) and C-AFM current maps in inverted scale (Figs. 5b, d, f) of AC/PANI (Figs. 5a, b), AC/PEDOT (Figs. 5c, d) and AC/PPy (Figs. 5e, f) composites

precipitation are shown in Fig. 4a – topography, Fig. 4b – current map and obtained by mechanical mixing in Fig. 4c – topography, Fig. 4d – current map, respectively. In the topography, the images NiO crystallites or precipitates are not admittedly seen. However, the

current maps clearly show the conductive spots (black areas) at the non-conductive background (white area). Current distribution images indicate the conductive spots in the xy -plane, which means that their maps show places where the conductive network of the AC is not covered by the additives and appears at the surface. The non-conductive spots indicate the presence of NiO at the surface of the AC matrix. It is obvious that the non-conductive part is dominating over a small amount of the non-covered, conductive areas. On comparing both the composites, we can note that the composite obtained by the chemical method is characterised by bigger conductive areas, especially at the grains' boundaries, contrary to the composite obtained by the mechanical way. This suggests a more homogeneous distribution of the NiO at the surface of the composite obtained by the mechanical process than by the chemical precipitation.

3.2. Structure of the carbon/polymer composites: In the following discussion, all the samples are treated as a conductive matrix of the carbon material mixed with or covered by the much less conductive polymer (PANI, PEDOT and PPy). Fig. 5 presents the topographies (Figs. 5a, c and e) and the current maps (Figs. 5b, d and f) of the AC/polymer composites. Fig. 6 represents the topography images obtained in the TappingMode[®] of the individual MWNTS deposited at the mica (Fig. 6a) and the MWNTS taken from the PANI (Fig. 6b), PEDOT (Fig. 6c) and the PPy (Fig. 6d) composite, deposited at the highly ordered pyrolytic graphite (HOPG) surface. We can see that the PANI and the PEDOT additives do not affect the topography of the bulk AC composites in a major way. The differences are inconsiderable and they are difficult to analyse because of the poorly defined activated carbons' morphology. Only in the PPy topography does an image somewhat bigger than typical AC grains appear, but it is difficult to analyse. In the case of the MWNTS composites, their analysis of form in which the polymer is attached to the carbon is much easier thanks to the well characterised nanotubes' structure. This is especially noted after

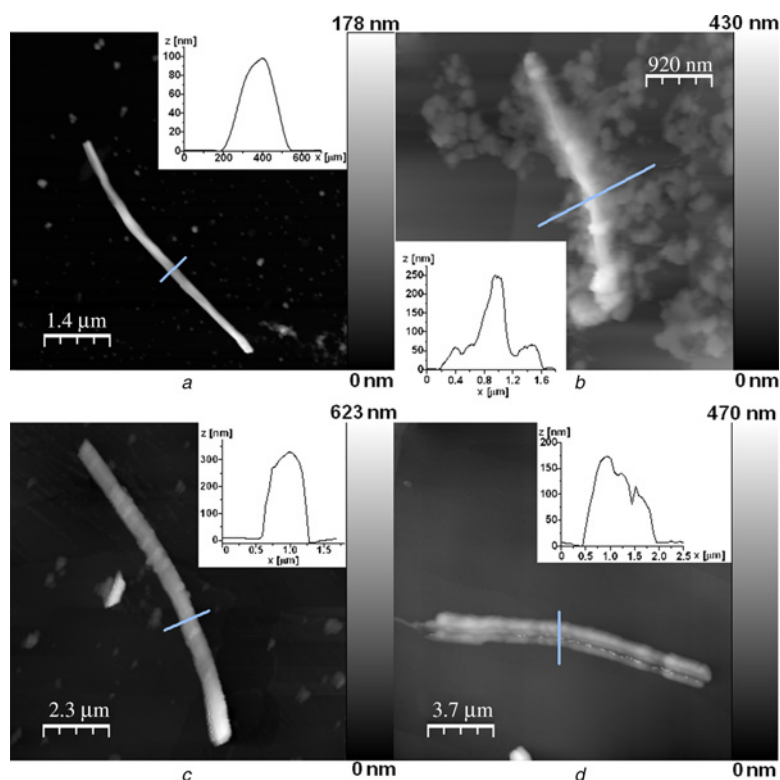


Figure 6 Topography of single multiwalled CNT deposited on mica and single CNT from the composite (Fig. 6a); with PANI (Fig. 6b); with PEDOT (Fig. 6c); with PPy (Fig. 6d) at HOPG

depositing the individual nanotubes on an atomically flat surface. However, this does not always reflect in the surface conductivity. Despite the fact that the topography images of the nanocomposites are difficult to analyse, the C-AFM current maps in all the cases give essential information about material distribution in the obtained composites.

The current map of the AC/PANI composite is shown in Fig. 5b. As seen, there is no current detection at the practically whole surface besides several negligible small conductive areas (black spots). That result suggests a nearly complete coverage of the AC by the polymer. This is confirmed by the topography of the single nanotube from the MWNTS/PANI composite presented in Fig. 6b. We can find that the PANI has a morphology similar to the spheres with a diameter of tens of nanometres. The same morphology of the PANI was reported earlier by Chen *et al.* [9]. PANI spheres are affixed to the nanotube and increase its height from a nominal 110–170 nm up to 250 nm. From the comparison of these two results, we can suggest the presence of a strong affinity of the PANI to carbon. This affinity enables covering the carbon by a thin layer of the polymer spheres which were incorporated into every free space and made the surface much less conductive, which can be proved by the C-AFM.

The PEDOT current map is shown in Fig. 5d. In contrast to the composite with the PANI, the PEDOT left some conductive parts on a surface (dark areas) and they are more or less linked with the grain structure of the composite (Fig. 5c). When we look at the way the PEDOT covers the single nanotube (Fig. 6c) we can find that the PEDOT makes thick, uniform shell surrounding nanotubes, increasing their diameter by up to more than 300 nm. This suggests that the AC grains were also quite fully covered by the PEDOT at the given stage of the polymerisation reaction. As a result, a majority of the grains became poorly conductive and probably only those spots of the carbon surface where the polymerisation process did not occur are highly conductive.

The current map of the AC/PPy composite is shown in Fig. 5f. The percentage of the surface with the current detection in the AC/PPy composite is much higher than in the AC/PANI and the AC/PEDOT composites, despite nearly the same amount of the polymer addition (about 50%) in the composite. There are some non-conductive spots within the conductive area at the top of the C-AFM current image, which are located at the grain boundaries. Fig. 6d shows the single CNT with the PPy polymer. We found that there is only a slight increase in the observed nanotube diameter by the addition of the polymer. PPy does not surround the whole nanotube, but it is visible as a fibre attached to the CNT. The same fibres should be attached to the AC grains, filling some free spaces between them.

4. Conclusion: In the case of conductive matrix/non-conductive (or less conductive) filler nanocomposites, imaging by means of the C-AFM is an efficient method to analyse the composite structure, the morphology, the homogeneity of the distribution and the electrical contact between the components of the composite. We have presented a novel method for the characterisation of the carbon composites by C-AFM, especially dedicated for the electrochemical capacitor electrodes. It was proven that the method is useful for the analysis of the homogeneity of the distribution of the non-conductive nanocomposite additives such as NiO, which are used as the pseudo-capacitive components. In the case of the polymer additives, the method shows the possibility to determine the coverage of the carbon material by the polymer. The method can also provide information on how the polymer is attached to the carbon materials such as the CNTs or activated carbon. It can help to find the proper preparation method of the nanocomposites with carbon as the main component. Also, it could be useful for the analysis of the electrical conductivity of the electrodes, which is the one of their crucial parameters. In particular, the utility of this method can be noted for the electrochemical capacitor and the lithium-ion batteries electrodes.

5. Acknowledgment: This work was supported by the Polish Ministry of Science and Higher Education under Project No. 62-213/13 DS PB.

6 References

- [1] Li Q.Y., Li Z.S., Lin L., *ET AL.*: 'Facile synthesis of activated carbon/carbon nanotubes compound for supercapacitor application', *Chem. Eng. J.*, 2010, **156**, pp. 500–504
- [2] Liu H.J., Wang X.M., Cui W.J., *ET AL.*: 'Highly ordered mesoporous carbon nanofiber arrays from a crab shell biological template and its application in supercapacitors and fuel cells', *J. Mater. Chem.*, 2010, **20**, pp. 4223–4230
- [3] Chen Q.L., Xue K.H., Shen W., *ET AL.*: 'Fabrication and electrochemical properties of carbon nanotube array electrode for supercapacitors', *Electrochim. Acta*, 2004, **49**, pp. 4157–4161
- [4] Burke A.: 'Ultracapacitors: why, how, and where is the technology', *J. Power Sources*, 2000, **91**, pp. 37–50
- [5] Yuan G.H., Jiang Zh., Aramata A., Gao Y.Z.: 'Electrochemical behavior of activated-carbon capacitor material loaded with nickel oxide', *Carbon*, 2005, **43**, pp. 2913–2917
- [6] Kalaji M., Murphy P.J., Williams G.O.: 'The study of conducting polymers for use as redox supercapacitors', *Synth. Met.*, 1999, **102**, pp. 1360–1361
- [7] Kiamahalleh M.V., Zein S.H.S., Najafpour G., Sata S.A., Buniran S.: 'Multivalled carbon nanotubes based nanocomposites for supercapacitors: a review of electrode materials', *Nano*, 2012, **7**, p. 1230002
- [8] Huang F., Chen D.: 'Towards the upper bound of electrochemical performance of ACNT@polyaniline arrays as supercapacitors', *Energy Environ. Sci.*, 2012, **5**, pp. 5833–5841
- [9] Chen F., Liu P., Zhao Q.: 'Well-defined graphene/polyaniline flake composites for high performance supercapacitors', *Electrochim. Acta*, 2012, **76**, pp. 62–68
- [10] Zhang K., Zhang L.L., Zhao X.S., Wu J.: 'Graphene/polyaniline nanofiber composites as supercapacitor electrodes', *Chem. Mater.*, 2010, **22**, pp. 1392–1401
- [11] Lota K., Khomenko V., Frackowiak E.: 'Capacitance properties of poly(3,4-ethylenedioxythiophene)/carbon nanotubes composites', *J. Phys. Chem. Solids*, 2004, **65**, pp. 295–301
- [12] Lei C., Wilson P., Lekakou C.: 'Effect of poly(3,4-ethylenedioxythiophene) (PEDOT) in carbon-based composite electrodes for electrochemical supercapacitors', *J. Power Sources*, 2011, **196**, pp. 7823–7827
- [13] Liu R., Cho S.I., Lee S.B.: 'Poly(3,4-ethylenedioxythiophene) nanotubes as electrode materials for a high-powered supercapacitor', *Nanotechnology*, 2008, **19**, pp. 215710
- [14] Frackowiak E., Khomenko V., Jurewicz K., Lota K., Beguin F.: 'Supercapacitors based on conducting polymers/nanotubes composites', *J. Power Sources*, 2006, **153**, pp. 413–418
- [15] Zhu C., Zhai J., Wen D., Dong S.: 'Graphene oxide/polypyrrole nanocomposites: one-step electrochemical doping, coating and synergistic effect for energy storage', *J. Mater. Chem.*, 2012, **22**, pp. 6300–6306
- [16] Rakhi R.B., Chen W., Alshareef H.N.: 'Conducting polymer/carbon nanocoil composite electrodes for efficient supercapacitors', *J. Mater. Chem.*, 2012, **22**, pp. 5177–5183
- [17] Snook G.A., Kao P., Best A.S.: 'Conducting-polymer-based supercapacitor devices and electrodes', *J. Power Sources*, 2011, **196**, pp. 1–12
- [18] Merino C., Soto P., Vilaplana-Ortega E., *ET AL.*: 'Carbon nanofibres and activated carbon nanofibres as electrodes in supercapacitors', *Carbon*, 2005, **43**, pp. 551–557
- [19] Shi H.: 'Activated carbons and double layer capacitance', *Electrochim. Acta*, 1996, **41**, pp. 1633–1639
- [20] Alekseev A., Efimov A., Lu K., Loos J.: 'Three-dimensional electrical property mapping with nanometer resolution', *Adv. Mater.*, 2009, **21**, pp. 4915–4919
- [21] Stadermann M., Papadakis S.J., Falvo M.R., *ET AL.*: 'Nanoscale study of conduction through carbon nanotube networks', *Phys. Rev. B*, 2004, **69**, p. 201402(R)
- [22] Li Ch., Thostenson E.T., Chou T.-W.: 'Dominant role of tunneling resistance in the electrical conductivity of carbon nanotube-based composites', *Appl. Phys. Lett.*, 2007, **91**, p. 223114
- [23] Alekseev A., Chen D., Tkalya E.E., *ET AL.*: 'Local organization of graphene network inside graphene/polymer composites', *Adv. Funct. Mater.*, 2012, **22**, pp. 1311–1318
- [24] Horcas I., Fernandez R., Gomez-Rodriguez J.M., Colchero J., Gomez-Herrero J., Baro A.M.: 'WSXM: a software for scanning probe microscopy and a tool for nanotechnology', *Rev. Sci. Instrum.*, 2007, **78**, p. 013705